

Properties and stability limits of an optimized mode-locked Yb-doped femtosecond fiber laser

Mohamed A. Abdelalim,^{1,3*} Yury Logvin,¹ Daa A. Khalil,² and Hanan Anis¹

¹*School of Information Technology and Engineering (SITE), University of Ottawa 800 King Edward, P.O. Box 450, stn A, Ottawa, Ontario, Canada, K1N6N5*

²*Department of Electronics and Communications Engineering, Faculty of Engineering, Ain Shams University, Cairo, Egypt*

³*Microwave Engineering Department, Electronics Research Institute (ERI), EL-Tahrir Street, Dokki, Cairo, Egypt.*

*Corresponding author: abosafe@site.uottawa.ca

Abstract: Stable mode-locked operation in a simple normal-cavity-dispersion laser oscillator that consists of only Yb-doped fiber and saturable absorber is studied. The Yb-doped fiber design parameters: group velocity dispersion (GVD), nonlinearity coefficient, bandwidth (Yb-BW), length and gain are considered to be the controlling parameters of the laser cavity. The pulse characteristics such as the temporal width, spectrum and pulse energy as a function of these elements are reported here. A pulse spectrum transition from M-like to Π -like and then to parabolic-like shape is observed with different values of the controlling parameters which are similar to that has been observed before in a solid-state laser. The stability limits in the domain of the Yb-BW and length are studied. The stability dependence on GVD, nonlinearity coefficient and gain of the Yb-doped fiber are elucidated. Moreover, the pulse instability dynamics beyond stability limits are found to be similar to that reported before for similariton.

© 2009 Optical Society of America

OCIS codes: (140.4050) Mode-locked lasers; (060.5530) Pulse propagation and solitons

References and links

1. S. Naumov, A. Fernandez, R. Graf, P. Dombi, F. Krausz and A. Apolonski, "Approaching the Microjoule Frontier with Femtosecond Laser Oscillators," *New J. Phys.* **7**, 216 (2005).
2. V. L. Kalashnikov, E. Podivilov, A. Chernykh, S. Naumov, A. Fernandez, R. Graf, and A. Apolonski, "Approaching the Microjoule Frontier with Femtosecond Laser Oscillators: Theory and Comparison with Experiment," *New J. Phys.* **7**, 217 (2005).
3. V. L. Kalashnikov, E. Podivilov, A. Chernykh, and A. Apolonski, "Chirped-Pulse Oscillators: Theory and Experiment," *Appl. Phys. B* **83**, 503 – 510 (2006).
4. F. O. Ilday, J. R. Buckley, W. G. Clark, and F. E. Wise, "Self-Similar Evolution of Parabolic Pulses in a Laser," *Phy. Rev. Lett.* **92**, 21, 213902 (2004).
5. J. R. Buckley, F. O. Ilday, T. Sosnowski, and F. W. Wise, "Femtosecond fiber lasers with pulse energies above 10 nJ," *Opt. Lett.* **30**, 1888-1890 (2005).
6. A. Chong, J. Buckley, W. Renninger, and F. Wise, "All-normal-dispersion Femtosecond Fiber Laser," *Opt. Express* **14**, 21, 10095-10100 (2006).
7. J. Buckley, A. Chong, S. Zhou, W. Renninger, and F. Wise, "Stabilization of high energy femtosecond ytterbium fiber lasers by use of a frequency filter," *J. Opt. Soc. Am. B* **24**, 1803-1806 (2007).
8. A. Chong, W. H. Renninger, and F. W. Wise, "Properties of Normal-Dispersion Femtosecond Fiber Lasers," *J. Opt. Soc. Am B* **25**, 140-148 (2008).
9. W. H. Renninger, A. Chong, and F. W. Wise, "Dissipative Soliton in Normal-Dispersion Fiber Lasers," *Phys. Rev. A* **77**, 023814 (2008).
10. N. Akhmediev, J. M. Soto-Crespo, and Ph. Grelu, "Roadmap to ultra-short record high-energy pulses out of laser oscillators," *Phy. Lett. A* **372**, 3124-3128 (2008).
11. G. P. Agrawal, *Nonlinear Fiber Optics*, 2nd ed., (Academic, San Diego, Calif., 1995).
12. N. Akhmediev and A. Ankiewicz, "Multisoliton solution of the complex Ginzburg-Landau equation," *Phy. Rev. Lett.* **79**, 4047-4051 (1997).

1. Introduction

Femtosecond fiber laser are attractive light sources as they offer many advantages such as compact size, maintenance- and alignment-free, and superior thermal handling. Their advantages arise from the light propagation in waveguide structure which results in an inherent stability and immunity against thermo-optical issues. Due to all these advantages, femtosecond fiber lasers have been the focus of intensive research in the last few decades. The latest progress demonstrates that femtosecond fiber lasers are a viable alternative to solid-state lasers beyond the confines of research laboratories.

Broadening of the pulse width using net positive group velocity dispersion (GVD) is a powerful way to increase the pulse energy. Drawing on this concept, higher pulse energies have been recently reported directly from large net normal GVD oscillators without external amplification; such as the so-called chirped pulse oscillator (CPO) [1-3], and self-similar laser [4]. A CPO produces highly chirped pulses which preserve the form during circulation in the cavity due to the weak dispersion map (DM) while the self-similar laser generates highly chirped pulses with notable breathing ratio due to strong DM in the cavity. This self-similar evolution suppresses the wave breaking by developing a monotonic frequency chirp during pulse propagation however the pulse energy is limited by overdriving the nonlinear polarization evolution (NPE) [5]. By reducing the strength of the NPE and using an inter-cavity filter providing additional self-amplitude modulation, stable pulses with notable high energy up to 13 nJ are generated [6, 7]. Such all-normal dispersion (ANDi) fiber laser containing an explicit spectral filter exhibits a variety of pulse shapes and evolutions [8]. The generated pulses from this ANDi fiber laser are found to balance not only phase modulation but also gain and loss thus they constitute dissipative solitons [9]. Recent theoretical study has found a region in parameter space where extremely high-energy stable dissipative solitons exist what provides a roadmap to design passively mode-locked laser oscillators with very energetic pulses directly from the cavity [10].

In this paper, we numerically demonstrate that a stable mode-locked pulse can be generated from a simple cavity consisting only of a normal dispersion Yb-doped fiber and a saturable absorber (SA). The mode-locked operation of the laser is modeled in the frame work of the extended Ginzburg-Landau equation. Numerical simulations show that stable pulses in the form of dissipative solitons can be generated in such a laser for some range of parameters. The Yb-fiber bandwidth, length and gain are considered as optimization parameters of the laser cavity. We show that depending on the Yb-doped fiber parameters the mode-locked pulses with the spectrum of different shapes can be generated. In addition, we demonstrate that there are stability limits in the space of the Yb-doped fiber laser parameters beyond which mode-locked pulse initially formed from the noise is unstable with respect to low-frequency perturbations.

2. Laser cavity model

The laser cavity structure used in this work is illustrated in Fig.1. It consists of Yb-doped fiber, WDM coupler with negligible single mode fiber (SMF) terminals lengths, polarization beam splitter for light output from the cavity as well as for providing mode-locking action through nonlinear polarization evolution (NPE), wave plate (WP) for controlling light polarization, and isolator for one direction light propagation.

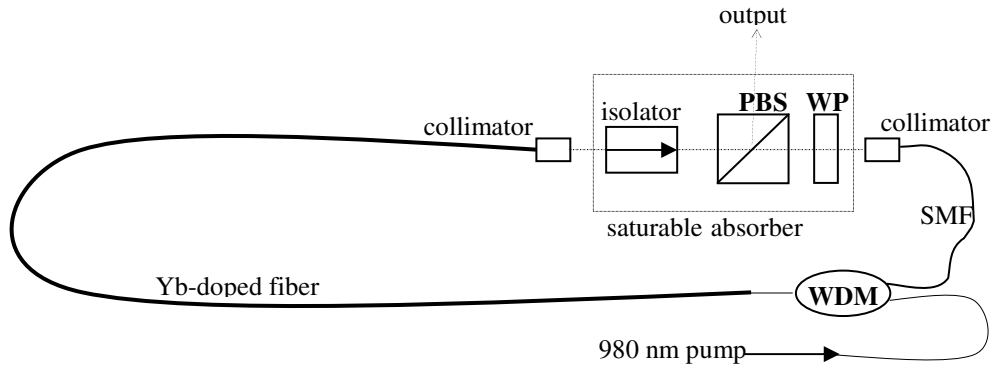


Fig. 1. Schematic view of the laser cavity: WDM – wavelength division multiplexer coupler, PBS – polarization beam splitter, WP – wave plate, SMF – single mode fiber.

Light propagation in the Yb-doped fiber is described by the Ginzburg-Landau equation for the complex amplitude A [11]:

$$\frac{\partial A}{\partial z} = -\frac{\alpha}{2}A - j\frac{\beta_2}{2}\frac{\partial^2 A}{\partial t^2} + j\gamma|A|^2A + \left(\frac{g_0}{1 + \frac{E_{pulse}}{E_{sat.}}} \right) \left(1 + \frac{1}{\Omega_g^2} \frac{\partial^2}{\partial t^2} \right) A, \quad (1)$$

where z is the propagation coordinate, t is the retarding time, $A(z, t)$ is the complex field amplitude, α is the linear loss taken as 0.04 m^{-1} , β_2 is the GVD parameter taken as $24000 \text{ fs}^2/\text{m}$, γ is the nonlinear parameter taken as $0.005 \text{ W}^{-1}\text{m}^{-1}$, g_0 is the small signal gain parameter (65 dB/m) with the parabolic frequency dependence and a bandwidth $\Omega_g = 40 \text{ nm}$, E_{pulse} is the pulse energy and $E_{sat.}$ is the gain saturation energy (3 nJ). Light propagation through polarizer has been modeled as intensity dependent transmission $T = 1 - l_0 / [1 + P_{pulse} / P_{sat}]$, where $l_0 = 0.5$ is the unsaturated loss, P_{pulse} is the pulse power and $P_{sat} = 12 \text{ kW}$ is the saturation power. Transmission characteristic corresponding to NPE can be described by sinusoidal function. However, for laser intensities below the over-driving point our transmission characteristic is quite good fit for NPE as it has been shown in many theoretical and experimental studies [4-8]. The total loss of the cavity has been taken as 10 dB corresponding to losses in all the different interfaces as well as to the light output from the cavity. The numerical method used is based on the split-step Fourier transform algorithm. As an initial condition, white noise has been used. Few thousand roundtrips are used to ensure that a stable mode-locked pulse operation has been reached.

3. Results and discussions

Stable pulses with linear chirp are generated numerically as depicted in Fig. 2. The temporal profile of the generated pulse is plotted in Fig. 2(a). A hyperbolic-secant shape function is fitting the temporal profile in Fig. 2(a). Obviously, the temporal profile is strictly fitted by sech-function so the generated pulse is considered a dissipative soliton [9]. The corresponding spectrum of the generated pulse illustrated in Fig. 2(b) is M-like shape spectrum and the linear chirp of the pulse is shown in Fig. 2(c). This linear chirp enables us to compress the pulse outside the laser cavity without deformation using an anomalous dispersion element until free-chirp pulse is reached [4]. Here the pulse chirp refers to the instantaneous frequency of the pulse.

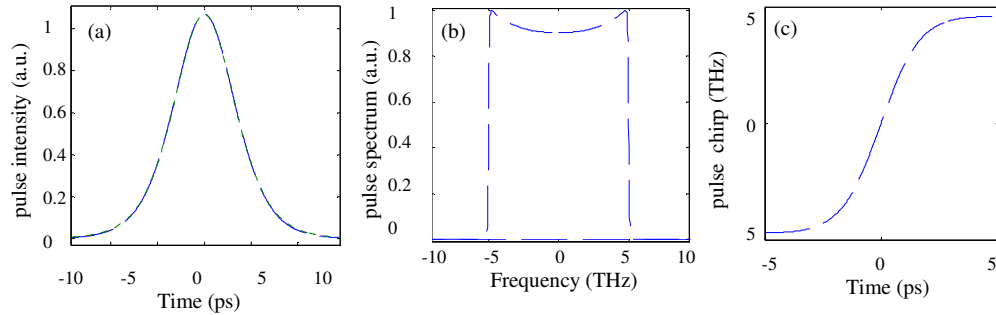


Fig. 2. The stable dissipative soliton at $g_0 = 65$ dB/m, Yb-BW = 40 nm, and Yb-length = 0.6 m. Temporal intensity profile fitted with sech-function (dotted), (b) Output power spectrum and (c) Pulse chirp.

The properties as well as the stability regions of the generated pulse are elucidated in the following subsections. First we consider the effect of the Yb-doped fiber parameters (dispersion, nonlinearity, gain bandwidth, length, and gain) on the pulse characteristics while the later subsections focus on the stability issues. The motivation to use the Yb-fiber gain bandwidth as a parameter is because the value for this parameter is quite different from one publication to another including experimental studies [6, 8]. We demonstrate how the region of stable mode-locked operation depends on the Yb-doped fiber parameters. Details of the mode-locked pulse instability beyond the edge of the stability region are also studied.

3.1. Variation of the Yb-doped fiber parameter

The following subsections display the variation of the pulse characteristics with the Yb-fiber GVD, nonlinearity, bandwidth, length, and gain respectively. The considered pulse characteristics for every Yb-fiber parameters are the temporal pulse profile and width, the spectrum pulse profile and width, the pulse chirp, and the pulse energy.

3.1.1 Yb-doped fiber GVD

We start by investigating the effect of the Yb-fiber GVD on the pulse characteristics. The results of the study are presented in Fig. 3. The temporal pulse profile keeps its shape as a hyperbolic-secant function. As shown in Fig. 3(a), the pulse becomes lower in amplitude and wider in width with increasing GVD as the GVD increases which is expected as a dispersion effect. However, the pulse spectrum changes from M-like shape to Π -like shape and then to parabolic like shape as the GVD increases, Fig. 3(b). As shown in Figs. 3(c) and (d) the temporal pulse width increases while the spectrum width decreases with increasing GVD which is consistent with Fig. 3-1. This is also confirmed by the decrease in pulse chirp shown in Fig. 3(e). On the other hand, the variation of the pulse energy with increasing GVD is quite weak as shown in Fig. 3(f).

3.1.2 Yb-doped fiber nonlinearity

Suffice it to say, the pulse characteristics are affected by increasing nonlinearity in a way similar to the situation when GVD decreases. Increasing nonlinearity keeps the temporal pulse profile as a hyperbolic-secant function with higher peaks, Fig. 4(a). In addition, it converts the spectrum profile from parabolic-like shape to Π -like shape and then to M-like shape, Fig. 4(b). The temporal pulse width slightly decreases with increasing the nonlinearity, Fig. 4(c), while the spectrum width increases significantly, Fig. 4(d). Obviously, the pulse chirp becomes stronger as the nonlinearity increases, Fig. 4(e). Again we have seen insignificant changes in pulse energy with nonlinearity change, Fig. 4(f), similar to the case of varying GVD, Fig. 3(f).

3.1.3 *Yb-doped fiber gain bandwidth (BW)*

We see in simulations quite a remarkable behavior when the gain BW changes, Fig. 5. As shown in Fig. 5(a), the temporal pulse profile remains of a hyperbolic-secant shape function, with pulse peak getting higher and the pulse width narrower. With decreasing gain bandwidth pulse spectrum becomes wider and the spectrum profile takes M-like shape as shown in Fig. 5b. Changes of the pulse width, Fig. 5(c), and of the spectral width, Fig. 5(d) with decreasing gain BW are related to the chirp of the generated pulse, Fig. 5(e), whose slope as well as maximum value increases with the decrease in BW. The impact of the BW on the pulse energy can be seen in Fig. 5(f). It is obvious that, there is a weak inverse proportionality between the BW and the energy of the generated pulse.

In the simulation, our laser configuration behaves as a function of the changing Yb-doped fiber gain BW similar to that of the ANDi fiber laser when the spectral filter bandwidth changes [7,8]. We see the same shortening of the mode-locked pulse and modification of the pulse spectrum from narrow parabolic to wide M-like shape. We also observe quite weak bandwidth dependence on the pulse energy as in [8]. Therefore, inverse dependence between the Yb-fiber BW and the mode-locked pulse width can be explained by the same mechanism as in ANDi laser [7, 8]: narrow bandwidth leads to pulse shortening due to cutting off the high- and low-frequency wings of the pulse. The only difference between our data and the results of [8] is that we do not see high spikes along the spectrum edges which could be attributed to the stronger contribution of the GVD in the pulse shaping in our case.

3.1.4 *Yb-doped fiber length*

The change of the Yb-doped fiber length causes variation simultaneously in the cavity GVD, nonlinearity, and total gain. Naturally, the length of the Yb-doped fiber makes an important impact not only on the pulse characteristics but also on the pulse stability as will be explained in the next section. It is clear from Fig. 6(a) that, the pulse intensity profile remains a hyperbolic-secant function with different peaks and pulse widths for different Yb-fiber length. Higher pulse peak with lengthening the Yb-fiber increases the pulse chirp and widens the pulse spectrum. As depicted in Fig. 4b, the effect of the length variation on the pulse spectrum profile is very weak and the spectrum remains as M-like shape for different values of the Yb fiber lengths except at short Yb length the spectrum profile becomes Π -like shape. Both the pulse and spectrum widths increase with increasing the Yb length, Figs. 4(c) and 4(d). However, the impact on the pulse width is weaker than that on the spectral width. The increase of both cavity GVD and nonlinearity with increasing Yb-fiber length is the cause for both pulse and spectrum widening [11]. As expected from the widening of the pulse spectrum, the maximum value of the linear chirp, shown in Fig. 6(e), increases with increasing the Yb fiber length. Increasing Yb fiber length produces more amplification; therefore it is obvious that pulse energy significantly increases with the length as shown in Fig. 6(f).

3.1.5 *Yb-doped fiber gain*

The variation of the Yb-fiber gain coefficient can be carried out experimentally by varying the input pumping power of the Yb-fiber. As the numerical results show, increasing the Yb-fiber gain keeps the temporal pulse profile as hyperbolic-secant shape with higher peak value (Fig. 5(a)), while it changes the spectrum profile of the generated pulse to M-like shape (Fig. 5(b)). The impact of the Yb-fiber gain on the temporal width of the pulse is different from that of the Yb-fiber length. As the Yb-fiber gain increases the nonlinearity increases and therefore the temporal pulse width becomes narrower as shown in Fig. 7(c). However, the increase of the Yb-fiber gain makes the spectrum wider as shown in Fig. 7(d). This spectrum widening with increasing the Yb-fiber gain is related to the increase of the generated pulse chirp as shown in Fig. 7(e). Also, the pulse energy grows naturally with Yb-fiber gain as

depicted in Fig. 7(f). Also, increasing the gain results in shorter pulse with wider spectrum and higher energy, as reported before in [8].

3.1.5 Analysis of the effects of the Yb-doped fiber parameters

The behavior of the temporal and spectral profile depends on whether GVD or nonlinearity dominates in the cavity [11]. The dominance of nonlinearity extensively increases the pulse chirp and hence widens the spectrum converting it to the M-like shape. In contrast, dominance of the GVD widens the temporal pulse and suppresses the spectral spikes of the pulse transforming the spectrum profile to parabolic-like similar to that of the ANDi laser [7,8].

It should be noted that similar transition in the mode-locked pulse spectrum (from M-like shape to Π -like shape and then to parabolic-like shape) has been previously reported in a solid-state laser source with increasing net cavity GVD [1, 2]. However, in fiber lasers a transition of the pulse spectrum from M-like shape to parabolic like shape directly without observing Π -like shape has been demonstrated [8]. Thus, our optimized Yb-doped fiber laser demonstrates ability to generate rich variety of spectral profiles including spectrum of Π -like shape.

The effect of the BW on the pulse characteristics is related to its amplitude modulation role [6-8], as the spectral clipping of the chirped pulse inside the cavity is mapped to time. Thus, decreasing the BW has an effect on the pulse characteristics, Fig. 5, which is similar to that obtained by increasing the nonlinearity, Fig. 4, and is consistent with what has been reported in [8]. Gain and Yb-fiber length only affect the pulse energy significantly while the other parameters have approximately no effect on the pulse energy. Lengthening the Yb-fiber has compound effect on the pulse characteristics because it increases both the GVD and the gain effects so each parameter has its own partial effect. Strictly speaking, lengthening the Yb-fiber noticeably increases the temporal pulse width as a result of the GVD and significantly widens the spectrum converting it to M-like shape. We have found that pulse energy is strongly affected by the Yb-fiber gain and length and it does not depend much on the GVD, nonlinearity and Yb-fiber gain bandwidth. Many tendencies found in our model, including mode-locked pulse dependence on the gain bandwidth, are similar to previously studied case of ANDi laser with spectral filter [8].

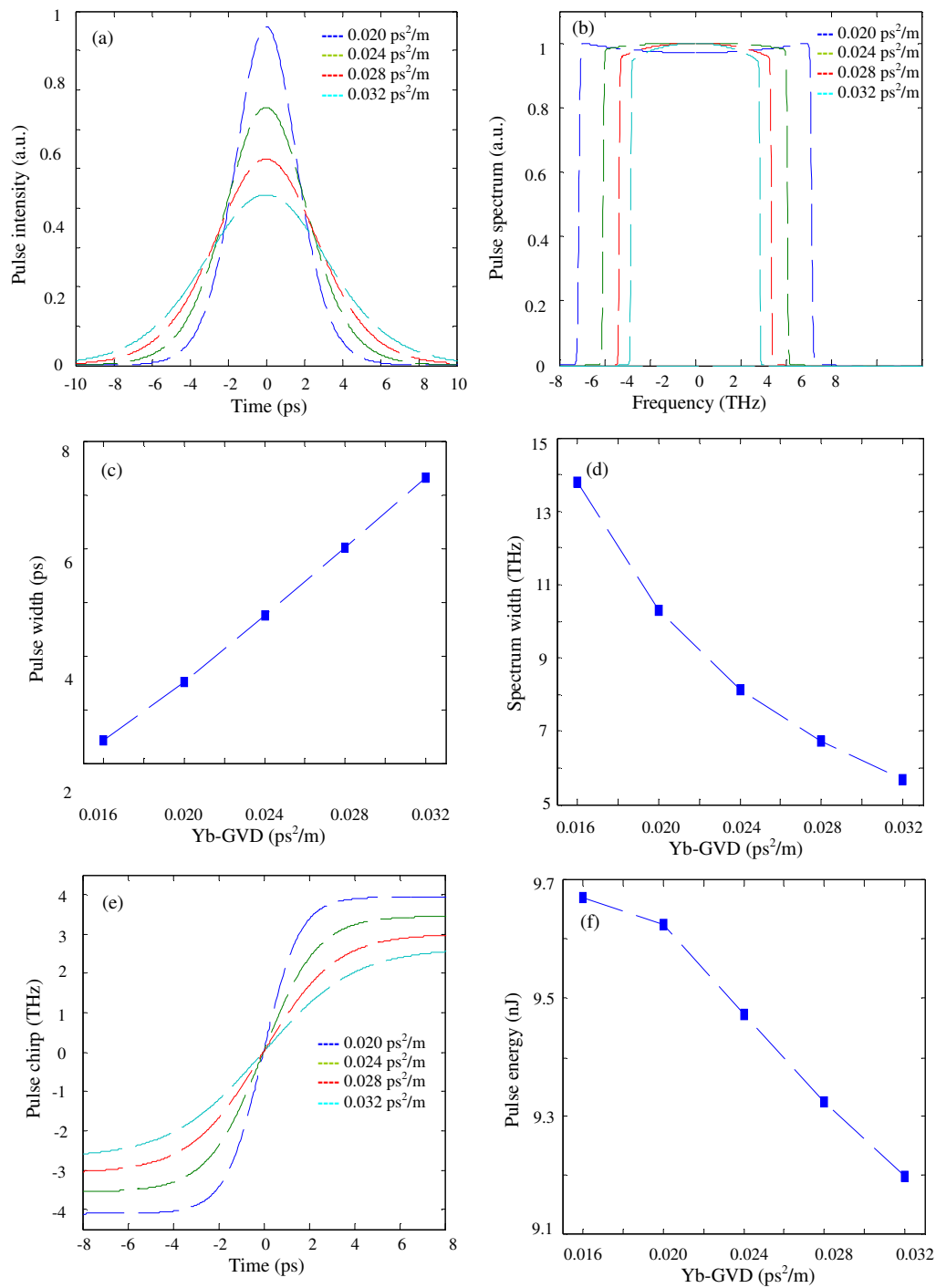


Fig. 3. The variation of the pulse characteristics: (a) the temporal pulse intensity, (b) the spectrum pulse intensity (c) Pulse width, (d) spectrum width, (e) pulse chirp, (f) pulse energy, with the Yb-GVD at $\gamma = 0.005 \text{ W}^{-1} \text{ m}^{-1}$, Yb-BW = 50 nm, $g_0 = 65 \text{ dB / m}$ and Yb-length = 0.6 m

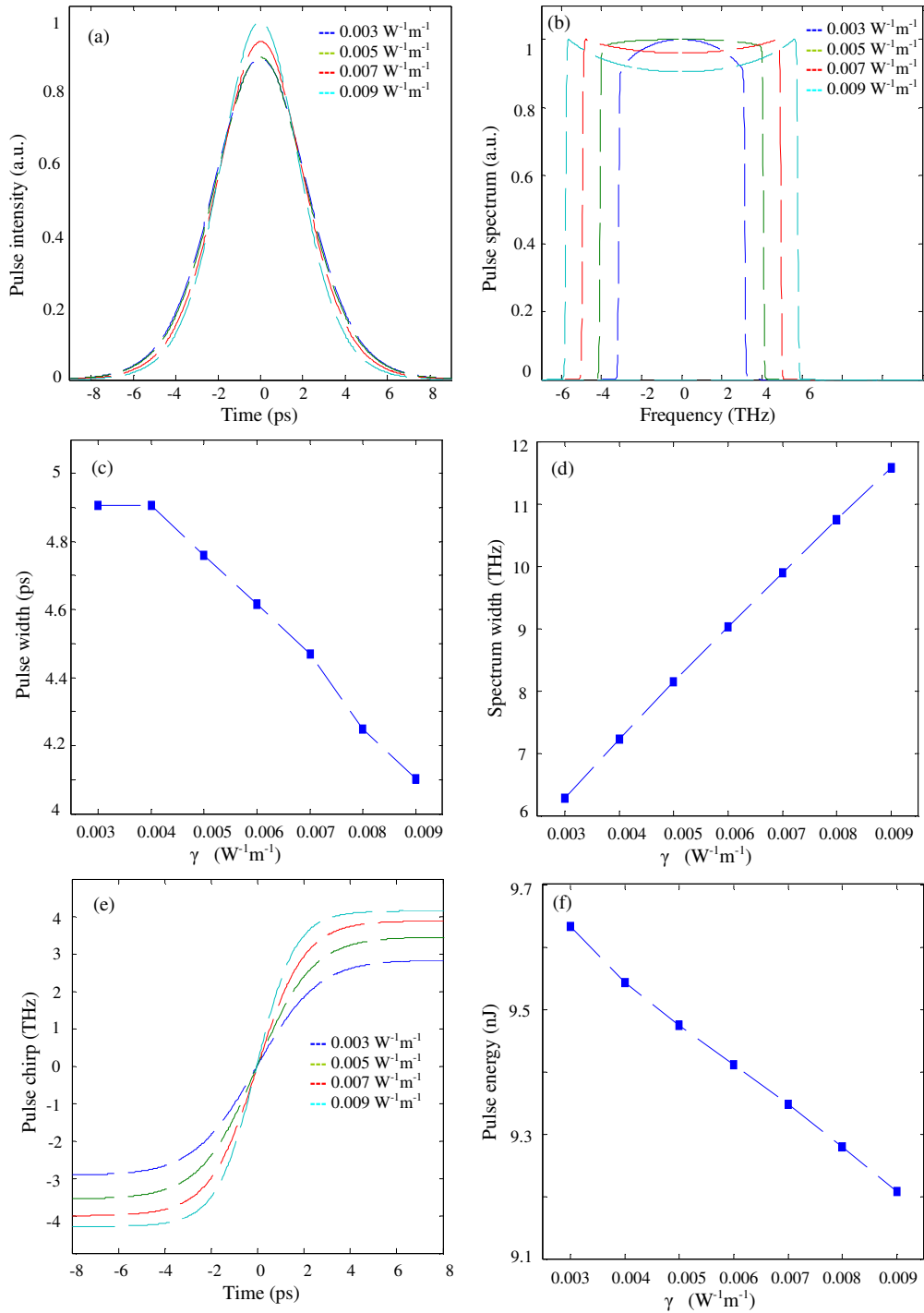


Fig. 4. The variation of the pulse characteristics: (a) the temporal pulse intensity, (b) the spectrum pulse intensity (c) Pulse width, (d) spectrum width, (e) pulse chirp, (f) pulse energy, with γ at Yb-GVD = 24000 fs^2/m , Yb-BW = 50 nm, $g_0 = 65 \text{ dB}/\text{m}$ and Yb-length = 0.6 m

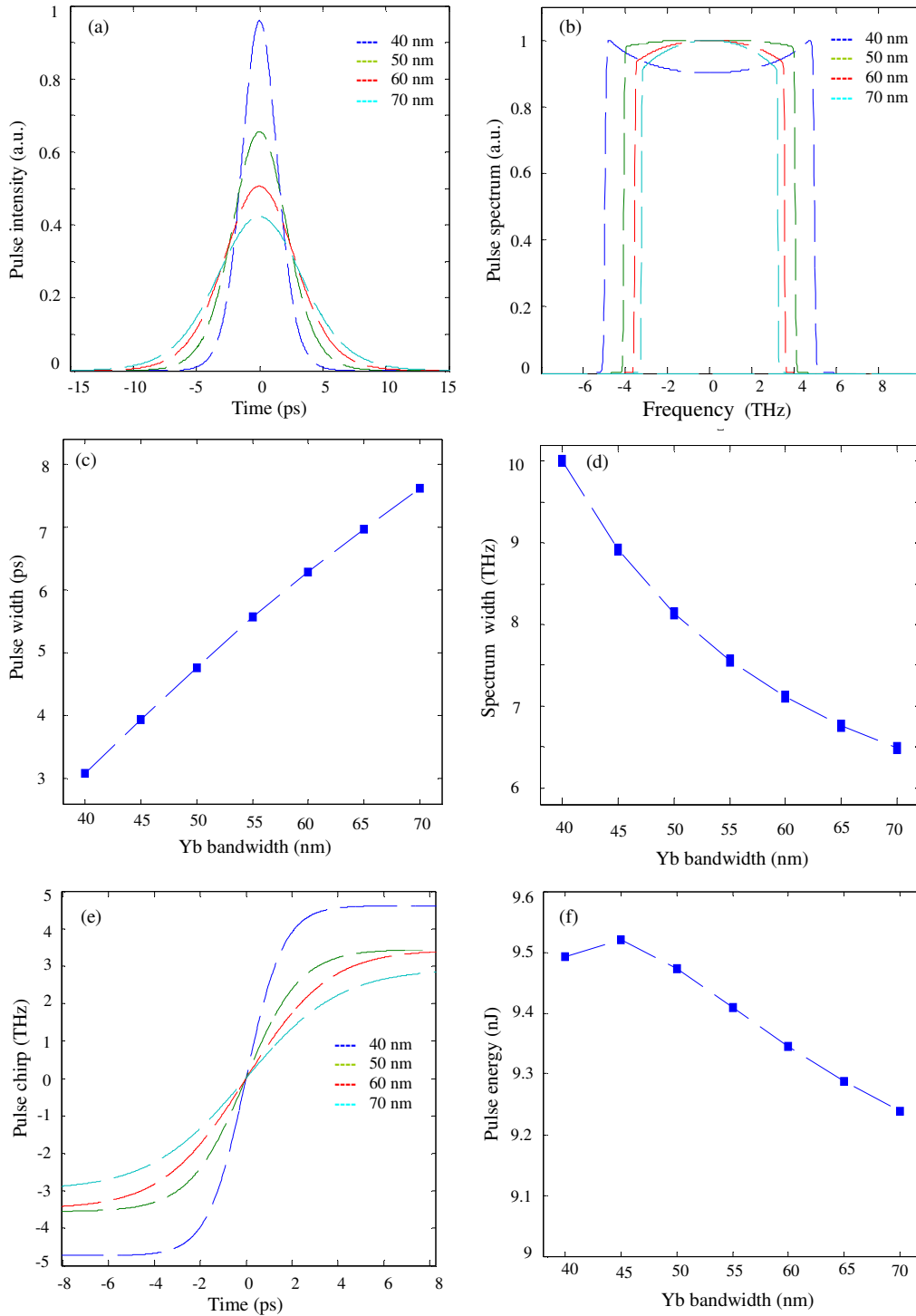


Fig. 5. The variation of the pulse characteristics: (a) the temporal pulse intensity, (b) the spectrum pulse intensity (c) Pulse width, (d) spectrum width, (e) pulse chirp, (f) pulse energy, with the Yb fiber bandwidth at Yb-GVD = 24000 fs²/m, $\gamma = 0.005 \text{ W}^{-1} \text{ m}^{-1}$, $g_0 = 65 \text{ dB/m}$ and Yb-length = 0.6 m

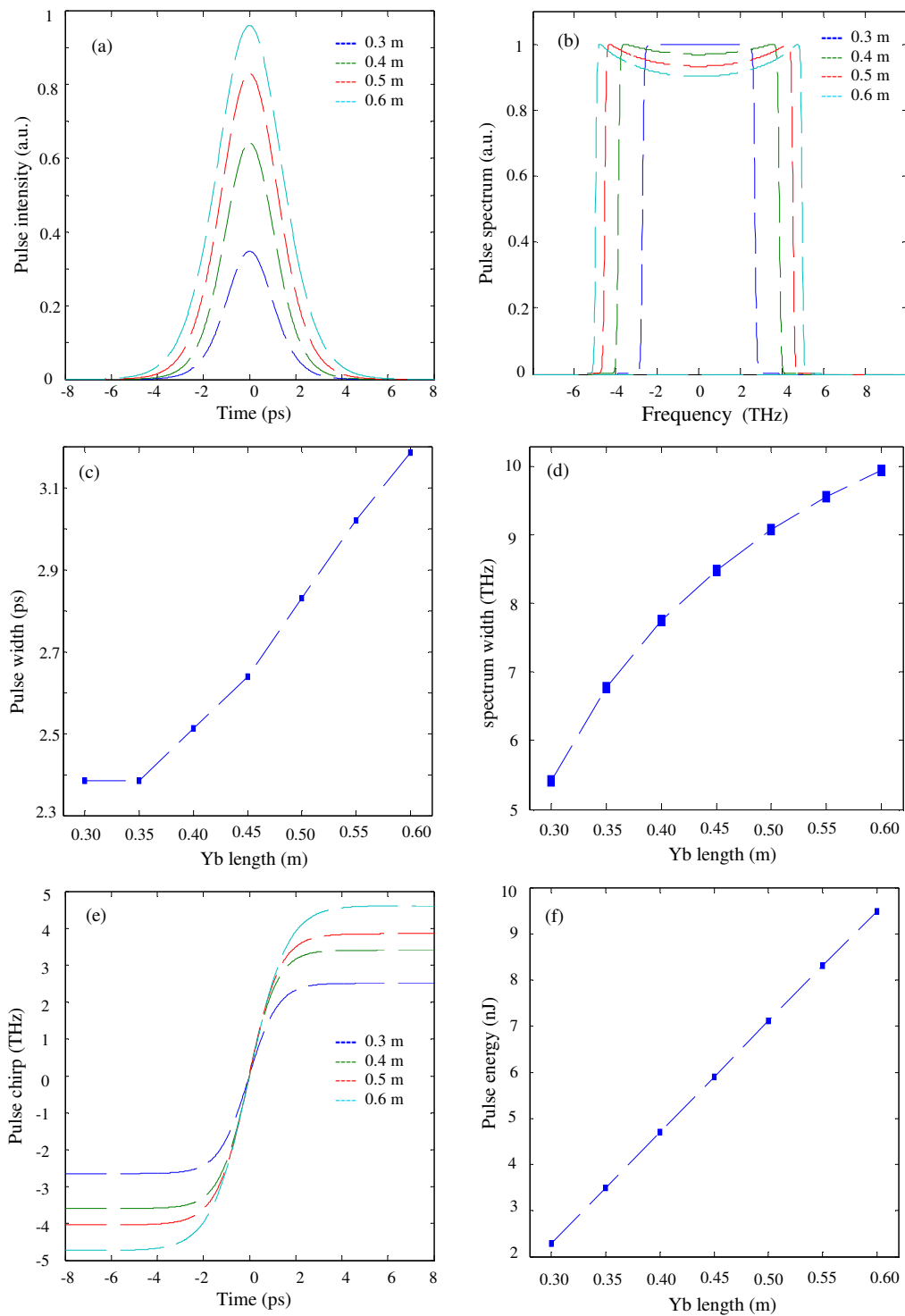


Fig. 6. The variation of the pulse characteristics: (a) the temporal pulse intensity, (b) the spectrum pulse intensity (c) Pulse width, (d) spectrum width, (e) pulse chirp, (f) pulse energy, with the Yb fiber length at Yb-GVD = 24000 fs²/m, $\gamma = 0.005 \text{ W}^{-1} \text{ m}^{-1}$ Yb-BW = 40 nm and $g_0 = 65 \text{ dB/m}$.

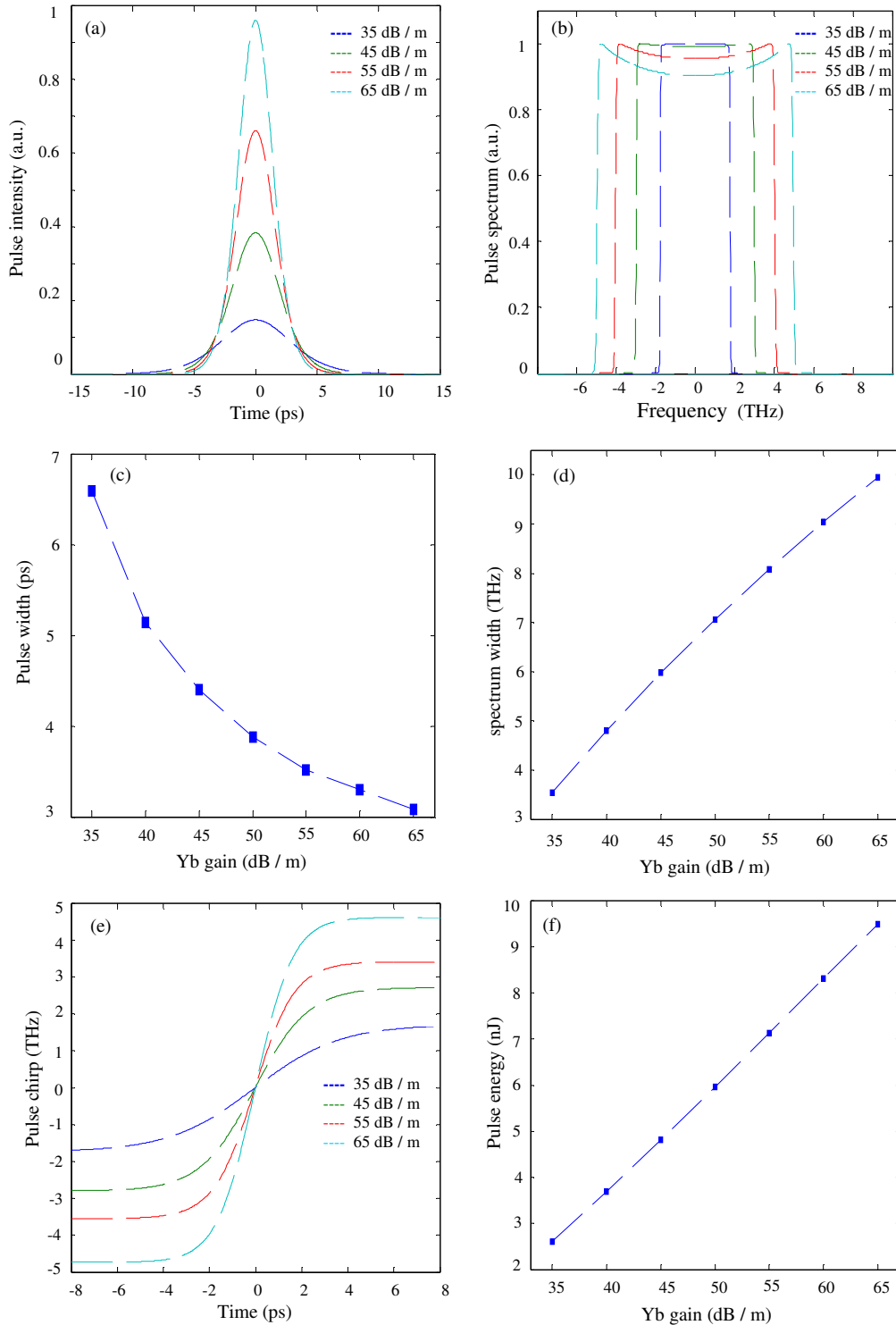


Fig. 7. The variation of the pulse characteristics: (a) the temporal pulse intensity, (b) the spectrum pulse intensity, (c) Pulse width, (d) spectrum width, (e) pulse chirp, (f) pulse energy, with the Yb fiber gain (g_0) at Yb-GVD = 24000 fs²/m, $\gamma = 0.005$ W⁻¹ m⁻¹ Yb-BW = 40 nm and Yb-length = 0.6 m.

3.2 Stability on the Yb-doped fiber parameters domain

In this section we study the instabilities which occur with the mode-locked dissipative soliton pulses developed from initial noise. The stability borders are identified on the plane of the Yb-doped fiber controlling parameters.

3.2.1 Yb-fiber BW and length stability area

First we study the instability threshold as a function of the Yb length and bandwidth. The calculations are limited in this part up to 1 m of the Yb-fiber length. This is because it is experimentally difficult to achieve uniform amplification inside the Yb fiber for longer length and the pulse may encounter some absorption. It is found that, as shown in Fig. 8, there is a wide area for the stable mode-locked operation denoted by "S". As we can see, the lower stability boundary is approximately linear, dotted line in Fig. 8. This means that as the length of the Yb-doped fiber increases, the minimum value of the BW required to get a stable pulse increases in approximately linear fashion. At short Yb-fiber length below 0.25 m for our particular cavity parameters, the gain is not sufficient to compensate for the cavity loss so this area is called "lossy" area, denoted by "L". The area denoted by "U" is the unstable area within which the initial mode-locking happens but the generated pulse is converted into chaos with time i.e. after many roundtrips. Snapshots of the instability dynamics in the U-area are discussed below.

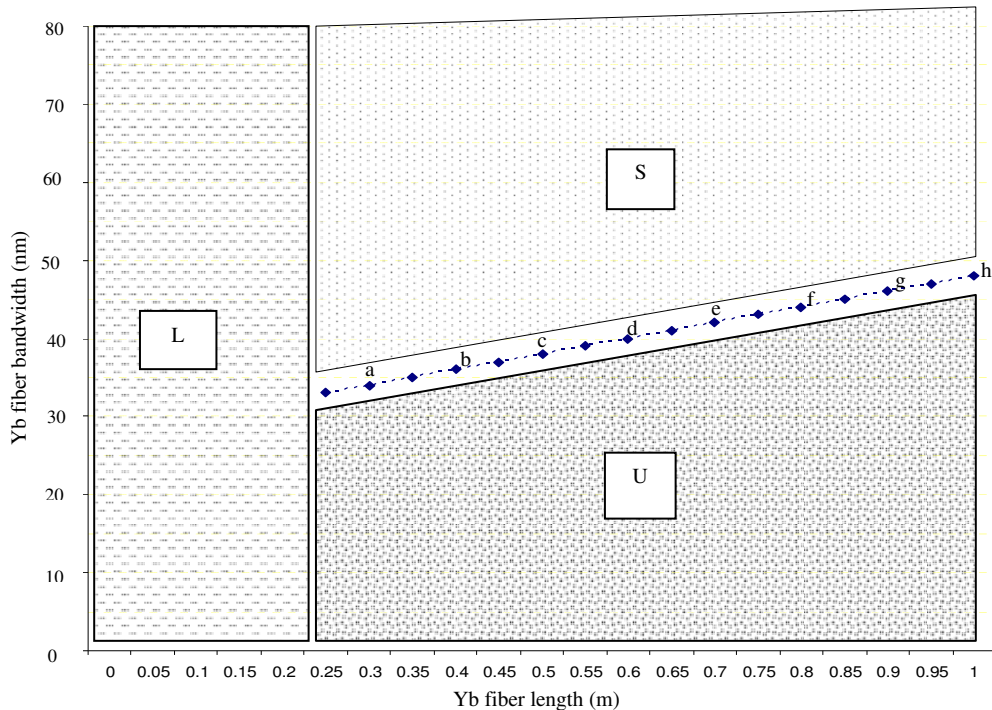


Fig. 8. Yb-fiber BW and length domain division according to the generated pulse state at $g_0 = 65$ dB/m

The pulse characteristics; temporal, spectrum, and chirp at different points denoted by a, b, c, d, e, f, g, and h on the edge of the stability area in Fig. 8 are plotted in Fig. 9. It can be seen that the

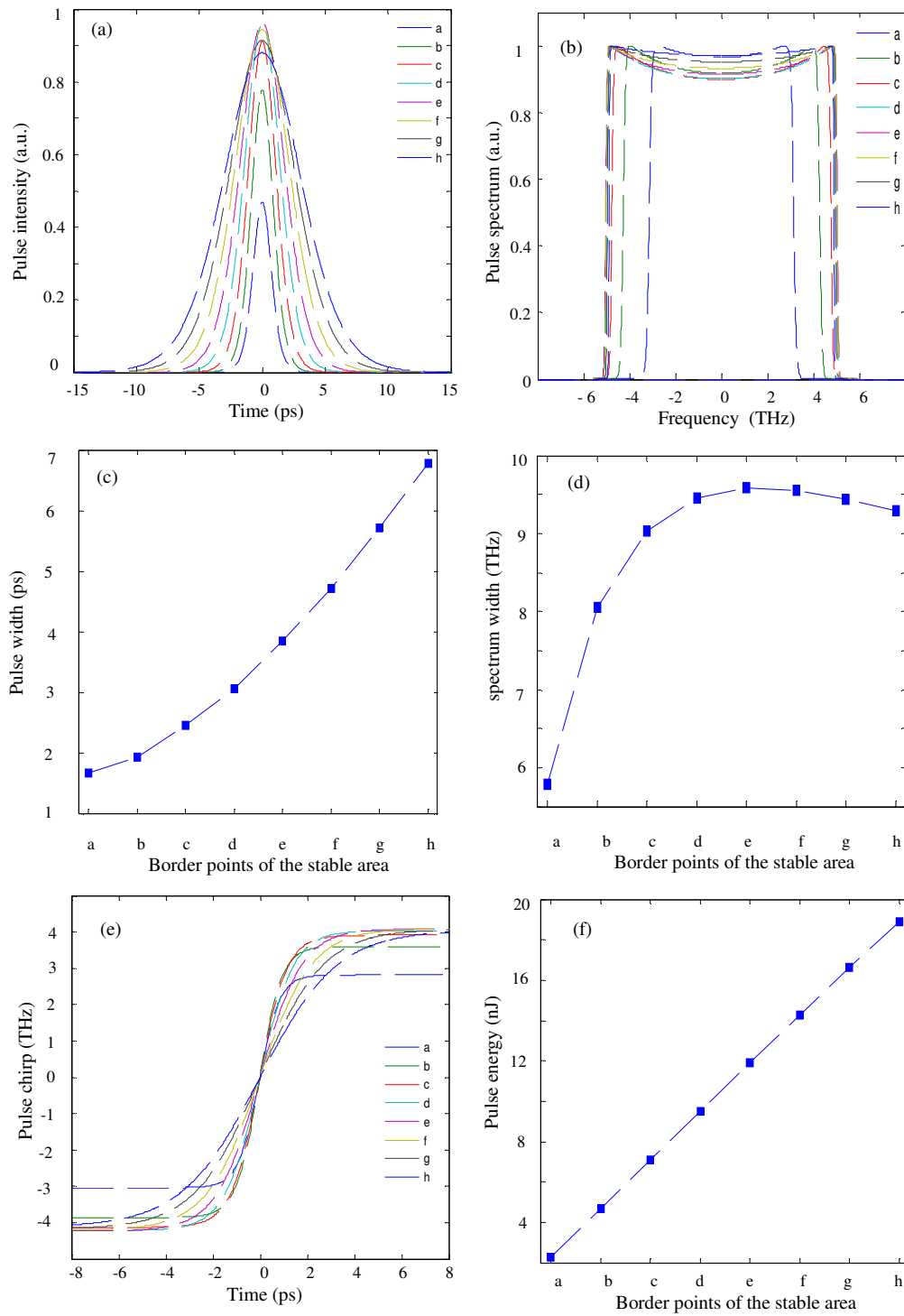


Fig. 9. Pulse characteristics on the edge of the stability region: (a) the temporal pulse intensity, (b) the spectrum (c) pulse width, (d) spectrum width, (e) pulse chirp, (f) pulse energy.

temporal shapes of the dissipative soliton pulses are of hyperbolic-secant profile with different widths. The spectrum profiles of the dissipative solitons on the edge of the stability region plotted in Fig. 9(b), remain approximately as M-like shape for any Yb-doped fiber length. The temporal pulse width increases monotonically from the lower value points to the higher value points as shown in Fig. 9(c). While the spectrum width increases first with the cavity length and get its maximum value approximately at point **e** after which the spectrum decreases as it is seen in Fig. 9(d). The pulse chirp also demonstrates extremum (this time, minimum) near point **e** as shown in Fig. 9(e). As expected the pulse energy increases along the instability boundary as shown in Fig. 9(f).

3.2.2 Yb gain impact on stability

The stability area “S” shown in Fig. 8 is affected by the changing the Yb-fiber gain. Fig. 10 demonstrates the displacement of the stability border as the Yb fiber gain changes. The stability area moves to the left-upper direction of the domain with increasing the Yb-fiber gain. This means that as the pumping increases, the minimum Yb-fiber length required to get stable mode-locked operation decreases and vice versa.

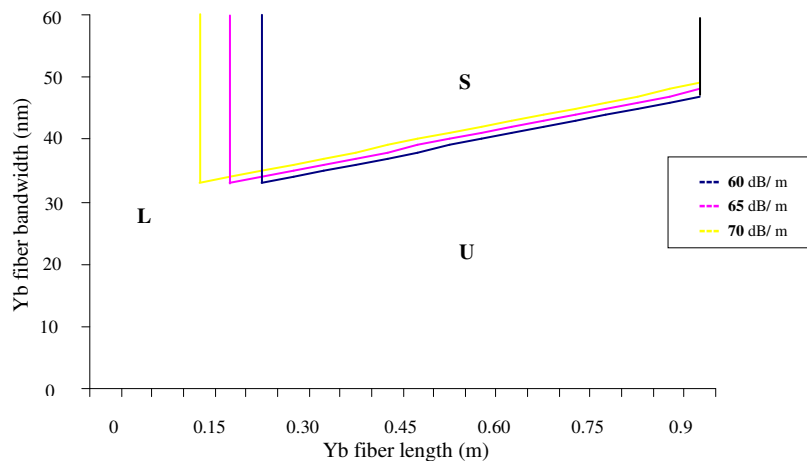


Fig.10. The edges of the stability area with different values of the Yb-doped fiber small signal gain (g_0)

Noteworthy here is that in our initial investigation for wider range of gain it is found other nontrivial dynamics like formation of coupled solitons [12]. This will certainly be a subject of further research.

3.2.3 Yb-GVD impact on stability

As the GVD increases the stability domain in the Yb-doped fiber parameters space broadens in a unique way, Fig. 11. We see that stable operation can be achieved at smaller Yb-fiber gain BW. It can be explained by the fact that GVD widens the temporal pulse profile and decreases spectrum width. In turn, the amplitude modulation resulted from the narrower Yb-fiber band width is required to destabilize the pulse. Since the GVD has approximately no effect on the pulse energy as explained above so it does not displace the vertical border of the lossy “L” area.

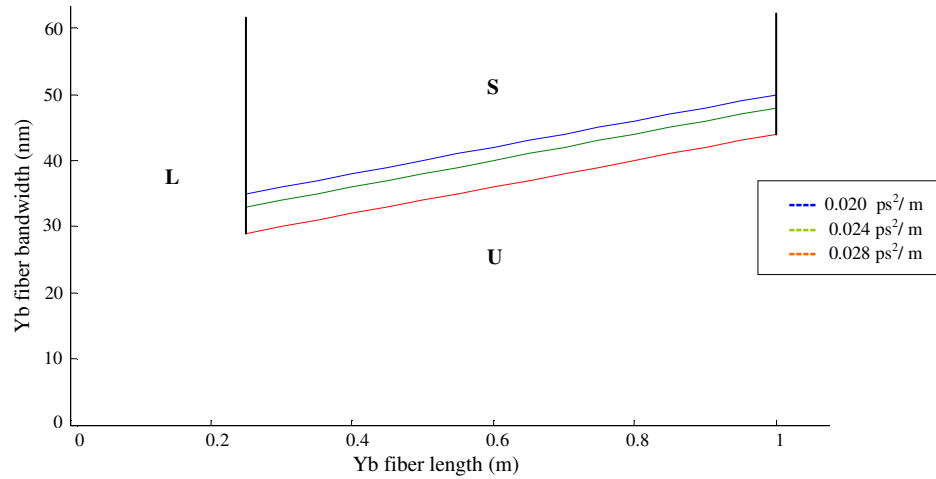


Fig.11. The edges of the stability area with different values of the Yb-doped fiber group velocity dispersion (GVD)

3.2.4 Yb-nonlinearity impact on stability

Figure 12 shows how the Yb-fiber nonlinearity shifts the stability border. It is seen that stability domain shrinks with the increase of nonlinearity. In contrast to the GVD case, the pulse spectral width grows with nonlinearity so that destabilization of the pulse occurs at larger Yb-fiber bandwidth. Again, the weak dependence of the pulse energy on the nonlinearity does not move vertical border of the stability domain.

It should be noted that another parameter which affects stability is the nonlinear modulator (saturable absorber) which is modeled by intensity dependent transmission through the polarizer in our case. We see in simulations that for weaker modulation, wider Yb-fiber bandwidth is necessary to keep pulse stable.

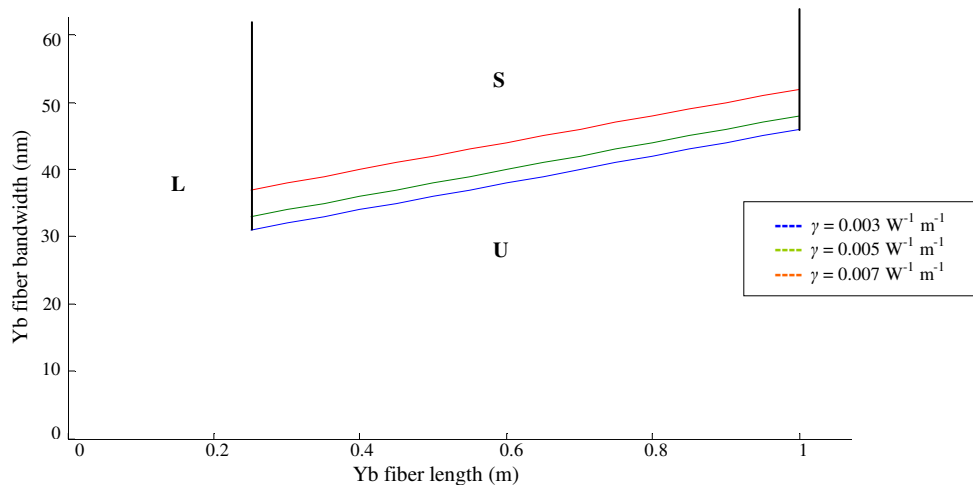


Fig.12. The edges of the stability area with different values of the Yb-doped fiber nonlinearity (γ)

3.2.5 Instability dynamics inside the unstable area

At any point in the area denoted by “U” in Fig. 11, a dissipative soliton that initially arises from laser noise collapses into chaos. It has been found that in this area, the pulse becomes unstable with time. An example of the instability dynamics of the initially formed dissipative soliton within “U” is illustrated in Fig. 11. After the pulse formation, the instability depicts itself through small ripples in the middle of the spectrum. These weak ripples become stronger with time until the pulse disappears and the chaos appears. This instability dynamics of the dissipative soliton with narrower Yb-doped fiber bandwidth is similar to those found previously for similariton regime [13].

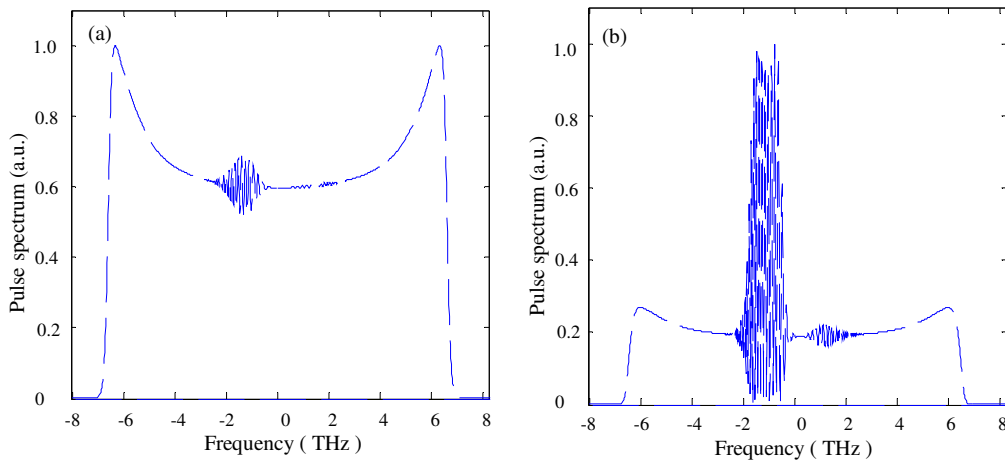


Fig. 13. The instability dynamics of the initially formed dissipative soliton after (a) 50 round trips and (b) 70 round trips of the pulse around the laser cavity

4. Conclusion

Numerical simulations demonstrate that a stable mode-locked pulse operation can be achieved in the relatively simple Yb doped fiber laser cavity comprising Yb-fiber with positive GVD and saturable absorber only. The Yb-doped fiber parameters; GVD, nonlinearity, bandwidth, length, and gain are considered as controlling elements of this cavity. Simulation reveals many stable pulses with different spectral profiles. A transition from M-like shape to Π -like shape and then to parabolic-like shape of the pulse spectrum is observed. This is similar to what has been reported before in a solid state laser. The impact of different cavity elements on the temporal and spectral characteristics of the pulse is presented. It has been found that GVD widens the pulse width and decreases the spectrum width while the nonlinearity does the opposite. Moreover, the amplitude modulation role of the Yb-fiber gain bandwidth is demonstrated. Lengthening the Yb-fiber widens both the temporal and the spectrum widths of the generated pulse due to the increase of both the group velocity dispersion and the gain of the cavity. Increasing Yb-fiber gain narrows the pulse and widens the spectrum due to nonlinearity effect. The domain within which a stable mode-locked pulse can be generated as a function of the laser parameters is identified. The characteristics of the pulse on the edge of a stable area are discussed. The shift of the stability border in response to change of the Yb-fiber parameters such as gain, GVD is elucidated. Finally, the instability dynamics of the pulse outside the stable regions is studied and it seems to be similar to that reported before for similariton.